Lumped-element modeling of density wave oscillations in two-phase hydrogen flows

T.L. Templeton [1], **K.I. Matveev** [1*] **and J.W. Leachman** [1]

[1] HYdrogen Properties for Energy Research (HYPER) Center, School of Mechanical and Materials Engineering, Washington State University, Pullman, WA 99164-2920 USA

[*]E-mail: matveev@wsu.edu

Abstract. Density wave oscillations (DWO) are one of the most common instability types in flow boiling systems. In liquid hydrogen (LH2) pipe flow with heat ingress, DWO can cause large fluctuations of temperature, pressure, void fraction, and flow rate in liquid hydrogen (LH2) pipe flow with heat ingress. Large fluctuations increase strain on systems and lead to unstable flow. Predicting the onset of these oscillations and their magnitudes is important for designing robust liquid hydrogen fuel lines. In this study, lumped-element modeling of density wave oscillations in two-phase hydrogen flow is undertaken to evaluate the instability threshold and limit-cycle oscillations in a single heated channel with different orientations. Nonlinear time-domain simulations are employed. The variable parameters include inlet liquid sub-cooling, flow rate, mean pressure, minor losses, and heat supplied to the channel wall. Non-dimensional stability plots using non-dimensional groups relating the variable parameters are presented to show examples of stable and unstable behavior. The results can assist designers and operators of liquid hydrogen transfer systems.

1. Introduction

Two-phase flow instabilities play a significant role in the behavior of flow boiling systems. Density wave oscillations (DWO) are one type of instability occurring when vapor is generated in pipe flow due to heat input [1-3]. Although DWOs have been studied with respect to boiling water reactors (BWR) [2], there is little information regarding DWO in cryogenic systems.

Cryogenic transfer lines that experience high heat leaks can be susceptible to two-phase flow instabilities [4, 5]. The heat influx to the liquid pipe flow can be on the order of 1 kW during the chill down process, which is enough to induce DWO [6]. The presence of cryogenic liquids in complex piping systems of rocket engines along with the high heating loads from combustion, can lead to boiling and the associated instabilities [7-9]. Liquid hydrogen fuel can act as coolant for the engine and vaporize prior to combustion that can also lead to two-phase flow instabilities [9]. In another common application, hydrogen fuel cells use gaseous hydrogen to function, but prefer liquid storage due to the low volumetric density of gaseous hydrogen [10]. Liquid hydrogen fueling of vehicles typically requires a phase change of the hydrogen to become usable, the heat leak and boiling that occur to achieve this phase transition can result in two-phase flow instabilities [10]. Liquid cryogen transfer can become unstable and extra thermomechanical strain on the equipment can arise in systems prone to DWO [11, 12].

DWO are dynamic instabilities caused by time lags in the system response to fluctuating values of pressure drop and mass flow rate which result in a positive feedback loop that can destabilize a system. This leads to sustained fluctuations in single and two-phase pressure drop, mass fluxes, and enthalpy flows. Flow oscillations impact fluid residence time in a pipe and thus the vapor generation [1, 13, 14]. Figure 1 shows a diagram of a typical system used for DWO analysis including a pipe with single- and two-phase regions. Flow properties will fluctuate in time in an unstable system even with a constant overall pressure drop and a fixed heat input to the pipe.

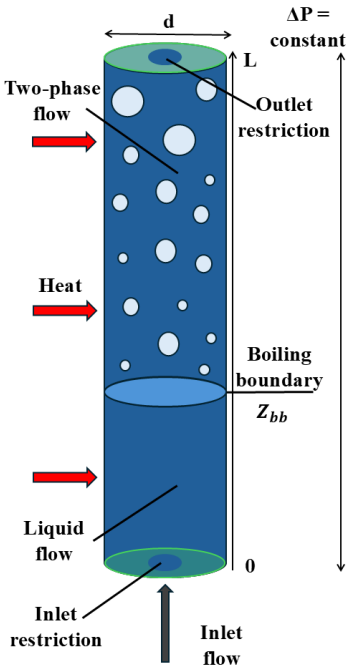

Figure 1. Schematic of a single heated channel showing single phase and two-phase regions

DWO can be better understood using several options for theoretical modeling. Computational fluid dynamics (CFD) is one approach which requires fine spatial and temporal discretization, that drastically increases the computational cost [15, 16]. Reduced order models (ROM) are another approach which are much less expensive computationally but also have lower fidelity due to additional approximations. However, using a validated ROM can efficiently provide valuable information.

In this paper, the reduced order model developed by Papini et al. [2], detailed in the next section, is applied to a liquid hydrogen system. Then, validation comparisons with experiments using both Freon-113 and liquid nitrogen are given. After, a parametric study for liquid hydrogen is presented including transient responses of the system. Finally, the dependence of oscillation amplitude on the supplied heat and the stability boundaries illustrating the effects of several system parameters is determined.

2. Theory

The model developed by Papini et al. [2], is a 2-node lumped parameter model (0D) that characterizes the single-phase and two-phase regimes in a single channel [2]. Assumptions include one-dimensional homogeneous flow, constant pressure drop across the overall system, fixed fluid properties at the inlet, and negligible sub-cooled boiling. The governing one-dimensional mass, energy, and momentum equations are as follows:

$$\frac{\partial \rho}{\partial t} + \frac{\partial G}{\partial z} = 0\,, \tag{1}$$

$$\frac{\partial (\rho h)}{\partial t} + \frac{\partial (G h)}{\partial z} = \frac{Q}{V}\,, \tag{2}$$

$$\int_0^L \frac{\partial G(z,t)}{\partial t} dz = \Delta P(t) - \Delta P_{acc} - \Delta P_{grav} - \Delta P_{frict}\,, \tag{3}$$

where ρ is the density, G the mass flux, h is the specific enthalpy, Q is the heat input, V is the volume, t is time, z is the axial coordinate, ΔP_{acc} is the accelerative pressure drop, ΔP_{grav} is the gravitational pressure drop, ΔP_{frict} is the frictional pressure drop, and ΔP is the total pressure drop. Mass and energy conservation equations are considered in the distinct regions while the

momentum equation is integrated across the entire channel. Wall dynamics are not included in the model and a constant heat flux from the wall in both regions is assumed. By integrating equations 1-3 along the pipe, ordinary differential equations for boiling boundary height Z_{bb}, exit quality x_{ex}, and inlet mass flux G_{in} will have the following form [2]:

$$\frac{dZ_{bb}}{dt} = \frac{2G_{in}}{\rho_f} - \frac{2QZ_{bb}}{(h_f - h_{in})V_{ch}\rho_f}\,, \tag{4}$$

$$\frac{dx_{ex}}{dt} = \frac{G_{in}v_{fg}x_{ex} - \Omega(L - Z_{bb})}{(L - Z_{bb})(v_f + v_{fg}x_{ex})\rho_{fg}b_5} + \frac{\gamma}{(\gamma - 1)(L - Z_{bb})b_5}\left[1 - \frac{\ln(1 + (\gamma - 1)x_{ex})}{(\gamma - 1)x_{ex}}\right]\frac{dZ_{bb}}{dt}, \tag{5}$$

$$(b_3 + Z_{bb})\frac{dG_{in}}{dt} = \Delta P(t) - \Delta P_{acc} - \Delta P_{grav} - \Delta P_{frict} - (G_{in} + b_1)\frac{dZ_{bb}}{dt} - b_2\frac{dx_{ex}}{dt}\,, \tag{6}$$

where ρ_f and ρ_{fg} are the respective liquid density and the evaporation density, h_f and h_{in} are the respective specific enthalpies of the liquid and at the inlet, V_{ch} is the volume of the channel, L is the length of the channel, Ω is the reaction frequency, v_f and v_{fg} are the respective specific volumes of the liquid and evaporation, γ is the density ratio, and b_1, b_2, b_3, and b_5 are modeling coefficients dependent on Z_{bb}, x_{ex}, and G_{in} resulting from the derivation of the model [2]. The pressure drop terms in Eq. 6 are given below:

$$\Delta P_{acc} = G_{ex}^2\left[\frac{x_{ex}^2}{\alpha_{ex}\rho_g} + \frac{(1 - x_{ex})^2}{(1 - \alpha_{ex})\rho_f}\right] - \frac{G_{in}^2}{\rho_f}\,, \tag{7}$$

$$\Delta P_{grav} = g\rho_f Z_{bb} + g(1 - \bar{\alpha})\rho_f(L - Z_{bb}) + g\bar{\alpha}\rho_g(L - Z_{bb})\,, \tag{8}$$

$$\Delta P_{frict} = \left(k_{in} + f\frac{Z_{bb}}{d}\right)\frac{G_{in}^2}{2\rho_f} + f\frac{L - Z_{bb}}{d}\langle\Phi^2\rangle\frac{\langle G_{2\Phi}\rangle^2}{2\rho_f} + k_{ex}\Phi_{ex}^2\,, \tag{9}$$

where G_{ex} and $G_{2\Phi}$ is the mass flux at the outlet and in the two-phase regime respectively, α_{ex} and $\bar{\alpha}$ are the void fraction at the exit and the void fraction averaged over the two-phase region, respectively, ρ_g is the density of the vapor, g is gravity, k_{in} and k_{ex} are the inlet and outlet resistance coefficients, d is the channel diameter, f is the single phase friction factor, and Φ^2 and Φ_{ex}^2 are the two phase friction factor multipliers, averaged over the two-phase region and at the exit, respectively. Several options for Φ^2 are available, and a sensitivity study comparing several models for Φ^2 is shown in the results [17-20].

The model is programmed into MATLAB such that the ordinary differential equations are discretized explicitly in time. The steady-state values are calculated initially and used for the first step. A small perturbation in the pressure drop, of 10 pascals, is provided at the start to disturb the flow. However, for small perturbations the limit cycle amplitude does not depend on the magnitude of the initial disturbance. Depending on the system parameters, the flow either approches a stable state or experiences sustained fluctuations. The two commonly used non-dimensional numbers that are employed for locating the stability boundary are listed below [21]:

$$N_{pch} = \frac{Qv_{fg}}{G_{in}Ah_{fg}v_f}\,, \tag{10}$$

$$N_{sub} = \frac{h_{in} - h_{sat}}{h_{fg}}\frac{\rho_{fg}}{\rho_g}\,, \tag{11}$$

where A is the cross sectional area. N_{pch} is the phase change number which is proportional to the ratio between heat input to the system and the inlet mass flux, and N_{sub} is the sub-cooling number which describes the level of sub-cooling at the inlet.

3. Results

3.1 Validation

Experimental measurements by Saha [22] for Freon-113 are compared with results from the lumped-parameter model over a range of heat fluxes and subcooling temperatures to produce a stability boundary for the test conditions presented by Saha [22]. The equations for the lumped-parameter model from section 2 were integrated and several two-phase friction multipliers were used to solve equation 9 [17-20]. Figure 2a shows a plot of the stability boundary using N_{pch} and N_{sub}. The different models demonstrate similar behavior and shape of the stability boundary with a shift along the N_{pch} axis. The Lockhart-Martinelli friction factor is selected for the liquid nitrogen validation case and the parametric study with liquid hydrogen due to the lowest deviations from experimental measurements (±25%). Figure 2b shows a comparison between frequency for the experimental data from Saha [22] and the chosen friction model. Approximate agreement is achieved between the experimental data and the model using the Lockhart-Martinelli friction factor.

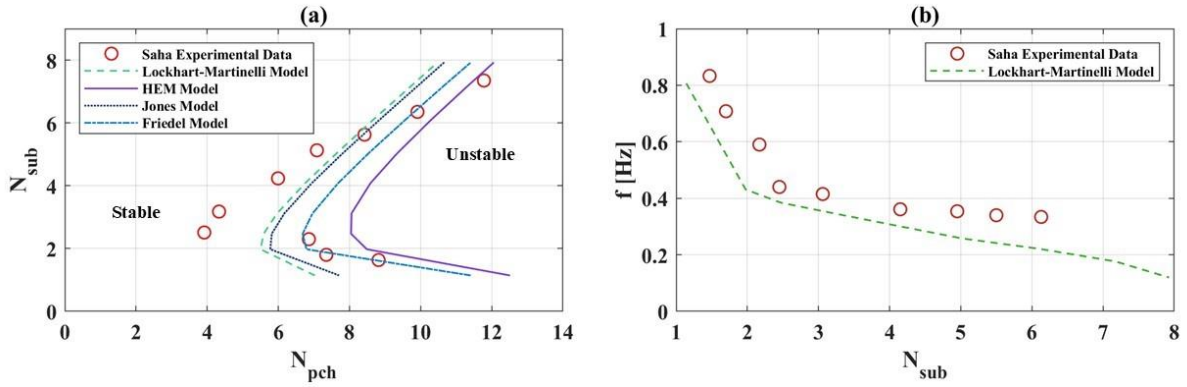

Figure 2. (a) Stability boundary for several two-phase friction models and experimental data for Freon-113 (b) Experimental frequency and modeling results with the Lockhart-Martinelli friction factor

Additional validation data is shown in Table 1 for a liquid nitrogen natural circulation loop experiment that was used to investigate DWO [23]. Table 1 includes the experimental parameters for each case, test data of the heat input at the stability boundary, the results from the model implemented in this paper using the Lockhart-Martinelli friction factor, and the percent error between the experimental and model results. The agreement between cases with a lower inlet resistance coefficient k_{in} is better than for higher k_{in} values. Given the simplified nature of the present model the agreement is deemed satisfactory. The deviations between the model and experimental test data presented by Ozawa [23] indicate that for this case about a 37% deviation in the heat fluxes will be observed in the stability boundary. Without further validation it is difficult to predict uncertainty for all practical systems.

Table 1. Comparison of experimental and modeled heat flux needed to induce DWO with liquid nitrogen.

	Case 1: $T_{sub} = 7K$, $P_m = 3\ bar, k_{in} = 330$	Case 2: $T_{sub} = 8K$, $P_m = 3\ bar, k_{in} = 580$	Case 3: $T_{sub} = 11K, P_m = 4.2\ bar, k_{in} = 330$	Case 4: $T_{sub} = 12K, P_m = 4.2\ bar, k_{in} = 580$
Experimental q	19.26 kW/m^2	23.89 kW/m^2	24.28 kW/m^2	28.73 kW/m^2
Model q	17.38 kW/m^2	15.05 kW/m^2	20.64 kW/m^2	21.29 kW/m^2
% deviation	−9.7%	−37%	−15%	−26%

3.2 Transient Response

Cryogenic transfer systems are accompanied by the chill in process and often operate outside of the nominal steady-state condition leading to transient behavior. Understanding the dynamic response is important in the design of effective cryogenic transfer systems [24]. Transient system parameters include the fluid being liquid hydrogen, a pipe length of 1 m, a pipe diameter of 1 cm, a mean velocity of 1 m/s, a mean pressure of 3 bar, an inlet temperature of 20 K, and variable heat input. A transition from a stable to an unstable regime occurs for a liquid hydrogen system as heat input is increased. Figure 3 shows a stable case with a heat ingress of 581 W which is very close to the stability boundary of 584 W which is significantly less than the heat ingress present for an uninsulated transfer line at room temperature.

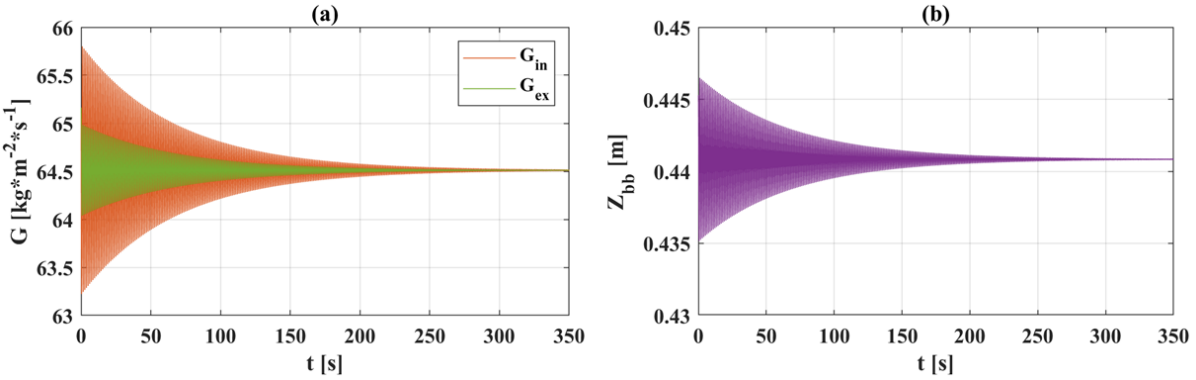

Figure 3. (a) Inlet and exit mass fluxes and (b) boiling boundary position for a stable case with a temperature of 20 K and a heat input value of 581 W

Limit cycle oscillations are characteristic to linearly unstable systems with non-linear damping [25]. Figure 4 shows the development and saturation of oscillations for the inlet and outlet mass flux as well as single and two-phase pressure drops. The limit cycle oscillations remain present over a particular range of heat input values before the system begins to display growing oscillations. In this case the range of heat input values that the limit cycle oscillations were present was 585 W to 639 W. If the heat input is above 639 W, the amplitude will not stabilize on a value and will instead grow with the boiling boundary reaching the system inlet/outlet at which point the model is no longer applicable. As the heat input increases from 585 W to 639 W, the amplitudes of the flow properties increase as shown in Figure 5. It should be noted that the limit cycle oscillations for the single-phase and two-phase pressure drops are out of phase (Figure 4b), an important mechanism for self-sustaining density wave oscillations [26]. The single-phase pressure drop can be linked with the inlet portion of the pipe and the two-phase pressure drop with the outlet. When the phase-shift of a feedback system is -180º it is inverted from the input

signal [27]. The inverted signal is fed back and subtracted from the input signal becoming positive feedback meaning that the input signal will not dampen and the system will be subject to reaching a limit cycle [27].

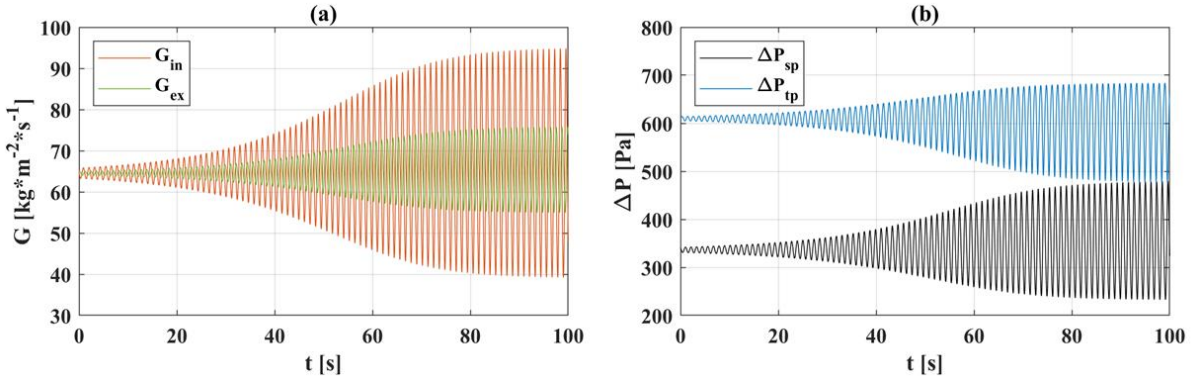

Figure 4. (a) Inlet and exit mass fluxes and (b) single-phase and two-phase pressure drop for an unstable case with a sub-cooled temperature of 20 K and a heat input value of 590 W

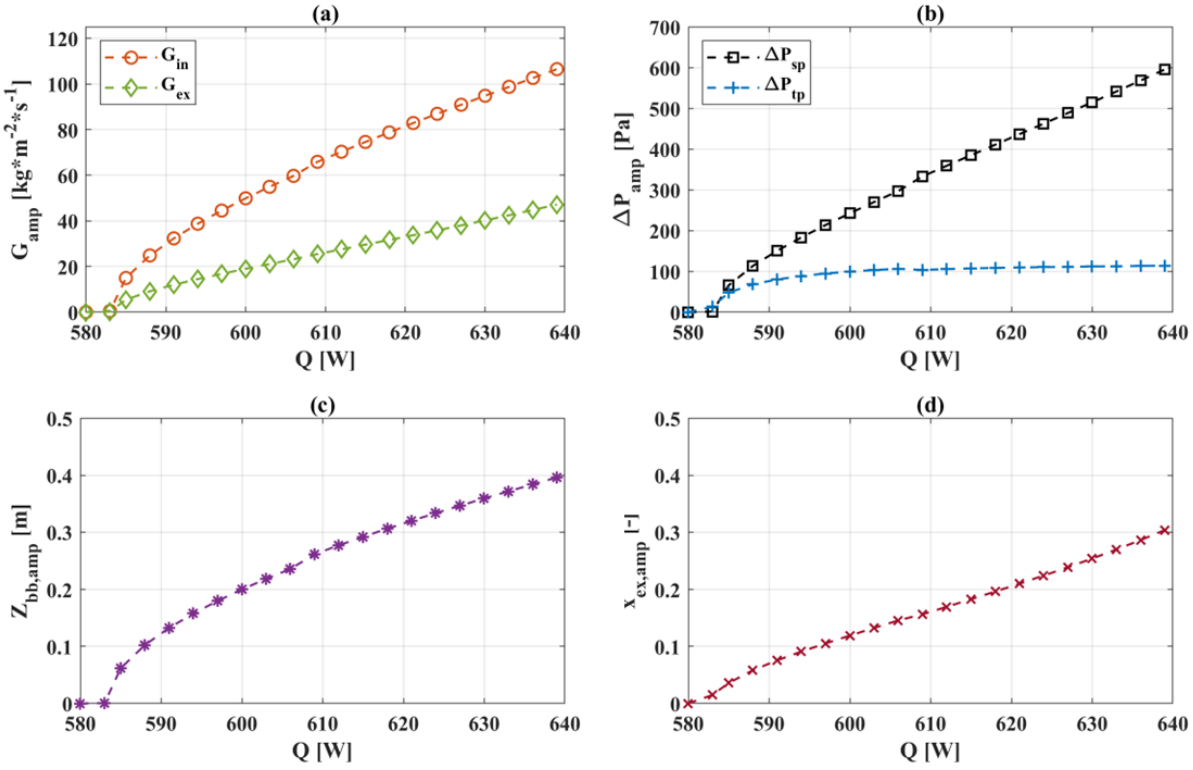

Figure 5. Change in amplitude across varying values of heat input for a temperature value of 20 K for (a) inlet and exit mass fluxes (b) single-phase and two-phase pressure drops (c) the boiling boundary height (d) the exit quality

3.3 Stability Boundary Study

Four variations of the system parameters listed in Table 2, have been explored to determine the effects on the stability boundary of the liquid hydrogen setup. Figure 6 shows the stability boundary for the system to stabilize for varying values of N_{sub}, a function of inlet temperature,

and the maximum value of N_{pch} is found which is a function of heat input. Figure 6a shows that increasing the mean pressure from the base case requires a lower N_{pch} value to destabilize the system, while decreasing the mean velocity shifts the boundary to a higher N_{pch}. It should be noted that this does not imply that a lower heat is needed to excite a high-pressure system. N_{pch} is influenced by the specific volume of the vapor (Eq. 11) which is higher at a low pressure resulting in the observed shift in N_{pch} In reality, larger heat input is needed to induce DWO at a higher mean pressure, which is consistent with previous studies [26,28]. A larger mean pressure causes the void fraction to reduce and consequently the frictional pressure drop as well, stabilizing the system.

Table 2. Variations of parameters for a liquid hydrogen system

	Base Case	Case 1:	Case 2:	Case 3:	Case 4:
$u_m[m/s]$	1	0.5	1	1	1
$P_m\ [bar]$	3	3	5	3	3
k_{in}	1	1	1	10	1
k_{ex}	1	1	1	1	10

Figure 6b shows the impact of the inlet/outlet resistance coefficients k_{in} and k_{ex}. Increasing the inlet resistance coefficient stabilizes the system and increasing the outlet resistance coefficient destabilizes the system. Increasing the inlet resistance causes the single-phase pressure drop to increase. The single-phase pressure drop is in phase with the inlet mass flux causing the oscillations to dampen [26]. Increasing the resistance at the outlet will raise the two-phase pressure drop which is out of phase with the inlet mass flux causing the oscillations to grow [26]. The behavior present in the resistance coefficient investigation is consistent with studies of other fluids [26]. From this analysis, k_{in} is found to have a greater impact on the system compared to k_{ex}.

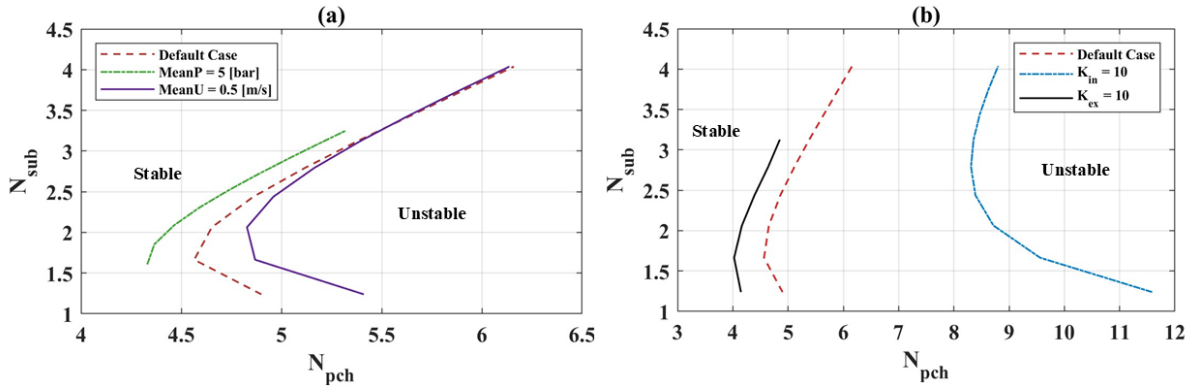

Figure 6. (a) Stability boundaries for 5 bar mean pressure and 0.5 m/s mean velocity and (b) stability boundaries for an increased resistance coefficient at the inlet and outlet together with a base setup using liquid hydrogen as the working fluid

4. Conclusion

In this study, a reduced order lumped-element model was used to analyze the transient response and produce a parametric case study for the stability boundary with liquid hydrogen as the working fluid. The model is validated against experimental data available for Freon-113 and liquid nitrogen showing approximate agreement generally within -37% for liquid nitrogen and ±25%

for Freon-113. From the stability boundary study using the two non-dimensional numbers N_{pch} and N_{sub} a combination of high k_{in}, low k_{ex}, high mean pressure, and high mean velocity promotes stability while limiting heat ingress into the system as much as possible. Future work in this area should include higher fidelity modeling techniques to achieve better agreement with experimental results and obtaining experimental measurements for liquid hydrogen.

References

[1] O'Neill L E and Mudawar I 2018 *International Journal of Heat and Mass Transfer* **123** 143-71
[2] Papini D, Cammi A, Colombo M, and Ricotti M E 2012 *Chemical engineering science* **81** 118-39
[3] Ambrosini W, Di Marco P, and Ferreri J C 2000 *International Journal of Heat and Technology* **18(1)** 27-36
[4] Bronson J C, Edeskuty F J, Fretwell J H, Hammel E F, Keller W E, Meier K L, Schuch A F, and Willis W L 1962 *Advances in Cryogenic Engineering* **7** 198-205
[5] Burke J C, Byrnes W R, Post A H, and Ruccia F E 1960 *Advances in Cryogenic Engineering* **4** 378-94
[6] Yuan K, Ji Y, and Chung J N 2007 *International journal of heat and mass transfer* **50(19-20)** 4011-22
[7] Zhu S, Fang S, Bao S, Zhi X, Wang K, and Qiu L 2024 *Renewable Energy* **236** 121488
[8] Popp M and Preclik D 1989 *25th Joint Propulsion Conference*
[9] Zhou C, Yu N, Wang J, Jin P, and Cai G 2021 *Acta Astronautica*, **189** 624-37
[10] Mori D, and Hirose K 2009 *International journal of hydrogen energy* **34(10)** 4569-74
[11] Gao Y, Wang Z, Li Y, Ma E, and Yu H 2024 *International Journal of Heat and Fluid Flow* **107** 109335
[12] Chen S, Chen X, Luo G, Zhu K, Chen L, and Hou Y 2018 *Applied Thermal Engineering* **144** 812-24
[13] Hurley P R 2023 Density-Wave Instability Characterization in Boiling Water Reactors under MELLLA+ Domain during ATWS *PhD Thesis* Virginia Polytechnic Institute and State University
[14] Kakaç S, and Bon B 2008 *International journal of heat and mass transfer* **51(3-4)** 399-433
[15] Dutta G, Zhang C, and Jiang J 2015 *Nuclear Engineering and Design* **286** 150-62
[16] Sharma S L, Buchanan J R, and De Bertodano M L 2020 *Nuclear Science and Engineering* **194(8-9)** 665-75
[17] Friedel L 1979 *European Two-Phase Flow Group Meeting*
[18] Lockhart W R 1949 *Chemical engineering progress* **45(1)** 39-48
[19] Martinelli R T and Nelson D B 1948 *Transactions of the American Society of Mechanical Engineers* **70(6)** 695-702
[20] Todreas N E and Kazimi M S 2011 *Nuclear Systems I: Thermal Hydraulic Fundamentals* (Boca Raton: Taylor & Francis)
[21] Ishii M 1971 Thermally induced flow instabilities in two-phase mixtures in thermal equilibrium *PhD Thesis* Georgia Institute of Technology
[22] Saha P 1974 Thermally induced two-phase flow instabilities, including the effect of thermal non-equilibrium between the phases *PhD Thesis* Georgia Institute of Technology
[23] Ozawa M, Asao Y, and Takenaka N 1993 *Instabilities in Multiphase Flows* (Boston: Springer)
[24] Johnson J and Shine S R 2015 *Cryogenics* **71** 7-17
[25] Mellodge P 2015 *A Practical Approach to Dynamical Systems for Engineers* (Cambridge: Woodhead Publishing)
[26] Boure J A, Bergles A E, and Tong L S 1973 *Nuclear engineering and design* **25(2)** 165-92
[27] Zumbahlen H 2008 *Linear Circuit Design Handbook* (Newnes)
[28] Guanghui S, Dounan J, Fukuda K, and Yujun G 2002 *Nuclear Engineering and Design* **215(3)** 187-98